

Adsorption and desorption studies of phenolic compounds on hydroxyapatite-sodium alginate composite

Rabia Benaddi^{a,b}, Faissal Aziz^c, Khalifa El Harfi^a, Naaila Ouazzani^{b,*}

^aLaboratory of Chemical Processes and Applied Materials (LPCMA), Polydisciplinary Faculty of Béni-Mellal University Sultan Moulay Slimane, BP 592, 23000 Béni-Mellal, Maroc, emails: r.benaddi@hotmail.fr (R. Benaddi), elharfi@yahoo.fr (K. El Harfi)

^bLaboratory of Water, Biodiversity and Climate Change Faculty of Sciences Semlalia, Cadi Ayyad University, BP 2390, Marrakech, Maroc, email: ouazzani@uca.ma

^cNational Center for Research and Studies on Water and Energy, Marrakech, 40000, MA, email: faissalaziz@gmail.com

Received 4 February 2020; Accepted 26 December 2020

ABSTRACT

In this work, elimination of phenol compounds from phenolic solutions by adsorption method in a column was studied. The adsorbent is polymer's beads, which are synthesized from a hydroxyapatite (HA) and sodium alginate (SA) by a method based on cross-linking process. Results showed that the synthesized adsorbent (HA/SA) can retain phenols with a high adsorption capacity (about 244 mg/g) and a slow reaction kinetics (about 4 h), which was described by a pseudo-second-order equation. The exploitation of the adsorption isotherm fitted well with the Freundlich model. It has been demonstrated that several parameters can influence the adsorption capacity of the tested adsorbent such as temperature, pH of solution and initial concentration of phenol. Results of regeneration of phenol showed that adsorbed phenol remains almost unstable and can be desorbed easily using only distilled water. The results also showed that desorption kinetics are more represented by the pseudo-second-order model. Results also demonstrated that the Freundlich model fitted better with the experimental data than with the Langmuir model, in addition, the adsorbent kept its high adsorption capacity for six cycles of adsorption-desorption. In the seventh cycle, the adsorption capacity decreases from 244 to 60 mg/g, due to saturation of adsorption sites.

Keywords: Adsorption; Desorption; Polymer's beads; Apatite; Phenolic solution; Reusability

1. Introduction

Phenols are mainly used by several industries, as a disinfectant, an extracting solvent in petroleum refining, resin and plastics manufacturing [1]. So phenols and its derivatives are discharged in various industrial waste water. At low concentrations, they are harmful to micro-organisms and at high concentrations, phenols affect human beings by denaturing proteins and destroying cell walls [2]. Various processes have been investigated by several researchers to remove phenolic compounds from wastewater [3–14]. Recently, there has been an increasingly great

interest in the literature devoted to the removal of aqueous organic species, such as phenols and its substitutes using adsorbents [15–21]. However, the high cost of many adsorbents limits its use. Several researchers have focused on the development of low-cost adsorbents [22–39] such as silicate gel and clay [22,23], bioadsorbents [24–26], scoria powder [32], or apatite [33–40]. In addition to the high cost of adsorbent, the main disadvantage of adsorption is the secondary pollution generated by the disposal of the used adsorbent. To overcome this disadvantage, there are many adsorbent regeneration techniques to re-establish the adsorbent capacity and to preserve, as much as possible,

* Corresponding author.

the initial structure of the used adsorbent. Thermal regeneration is among the most widely employed desorption methods. However it employs high-temperature oxidation for desorption of pollutant, which leads to the loss of adsorbent properties [41]. Chemical regeneration is very expensive because of the high cost of solvents. Hence the objective of this work is to synthesize and characterize new low-cost adsorbent materials for phenolic molecules that could allowing desorption using only distilled water without any thermal treatment or chemical regeneration. Adsorption–desorption kinetics of process and the effect of several parameters on the equilibrium of phenol adsorption were thoroughly studied.

2. Materials and methods

2.1. Adsorbents description

Natural phosphate rock (NP) was collected from Khouribga phosphate mine (Morocco), which is considered as the most important phosphate productive region in the world. The sample is pre-treated to remove impurities associated with phosphate minerals. After washing, phosphate particles, whose diameter ranged between 100 and 400 μm , have been chosen. Particles of phosphate were dried at 100°C and sieved to reduce the granulometry to less than 200 μm . The chemical composition of NP is P_2O_5 (30.24%), CaO (53.88%), SiO_2 (2.96%), F (3.78%), Al_2O_3 (0.57%) and Na_2O (2.20%). Elemental analysis of the main constituents of rock phosphate was carried out using an ICP-AES spectrometer (ULTIMA, REMINEX – RESEARCH CENTER, Guemassa Mine – BP 469 – Marrakech, Morocco).

The hydroxyapatite (HA) was synthesized by a principle based on dissolution of natural phosphate in the nitric acid [42]. A mass of 30 g of natural phosphate was introduced into a 2-L reactor containing a volume of 500 mL of distilled water and 20 mL of nitric acid solution (65%). The reaction mixture was kept under continuous stirring using a magnetic agitation for a period of 24 h at $\text{pH} = 2$ and at room temperature. After dissolution of natural phosphate, the obtained mixture was filtered under vacuum. The filtrate was then neutralized with a volume of 200 mL of ammonia (25%). The pH value of the mixture was adjusted at $\text{pH} = 10$ to avoid the formation of hydrogenphosphate. The precipitate formed was matured with stirring for 72 h. At the end of the maturation period, the filtered precipitate was washed with distilled water, and then dried at 100°C overnight. The chemical composition of HA is P_2O_5 (36.84%), CaO (57.6%), SiO_2 (0.78%), Al_2O_3 (1.41%) and Na_2O (2%). Elemental analysis of the main constituents of apatite was carried out using an ICP-AES spectrometer (ULTIMA, REMINEX – RESEARCH CENTER, Guemassa Mine – BP 469 – Marrakech, Morocco).

Hydroxyapatite-sodium alginate composite beads (HA/SA) were prepared by dripping method as described by Aziz et al. [43]. Briefly, 1 g of sodium alginate was dissolved in 50 mL of distilled water to produce a viscous solution. 0.125 g of hydroxyapatite (HA) was added into the corresponding SA solution under constant stirring during 2 h until the production of a homogeneous dispersion. Under magnetic stirring, the mixture solution was introduced drop by drop using a 10 mL syringe into 50 mL of calcium

chloride solution (1 g/L), the solution was sealed in the shade to solidify (during 24 h). The coagulated beads were then washed several times with distilled water and stored in distilled water until their use. Sodium alginate without hydroxyapatite (SA) was also prepared by adopting the same method used for the preparation of HA/SA but without adding hydroxyapatite to the SA solution in order to evaluate the effect of hydroxyapatite in the adsorbent structure.

2.2. Adsorbate

The used phenol (Sigma-Aldrich, Baden-Württemberg, Germany, purity = 99%) was not subjected to any prior treatment. The phenol stock solution (1 g/L, $\text{pH} = 6.20$) was prepared for each procedure.

2.3. Materials characterization

Scanning electron microscopy analyses were carried out by an apparatus type “Tescan Vega 3”. The adsorbent was previously metalized with carbon to ensure electrons conditions and also to avoid the effects of charge. The structure of the adsorbent was determined using X-ray powder diffractometer Rigaku (Center of Analysis and Characterization, Faculty of Sciences Semailia, Cadi Ayyad University, BP 2390, Marrakech, Morocco) with an analysis time of 100 min at room temperature. Infrared spectrum of the adsorbents was obtained by Fourier transform spectrometer Vertex 70, the pellet was obtained by crushing 0.001 g of samples with 0.099 g of KBr.

2.4. Sorption experiments

Sorption experiments were carried out in a cylindrical column made of glass of 4 cm internal diameter and 20 cm length. The column was filled with 3 g of the prepared adsorbent. Aqueous phenolic solution containing a known phenol concentration (100 mg/L) was filled in a reservoir of 500 mL, to assure a negligible change in the volume of the liquid level during the time. At room temperature, the solution was passed through the bed via peristaltic pump at constant flow rate of 1.7×10^{-3} L/s. At different time intervals, samples were collected from the reservoir solution until reaching the equilibrium. The determination of the residual concentration of each sample after filtration was carried out by spectrophotometer (M501 Camespec) at a wavelength $\text{max} = 270$ nm.

The adsorption capacity of phenol was obtained at different cycles using the equation:

$$q_e = \frac{(C_0 - C_e)V}{m} \quad (1)$$

where V : volume of solution (mL); m : mass of adsorbent (g); C_0 : initial concentration of phenol in solution reservoir (mg/L); C_e : equilibrium concentration of phenol in solution reservoir (mg/L).

At the end of the adsorption reaction, the remaining aqueous solution was drained off from column that was then washed with distilled water to remove phenol.

For desorption reaction of phenol from adsorbent, the solvent pumped into the column was maintained at constant temperature and at a fixed flow rate of 1.7×10^{-3} L/s. Solution samples were collected at different time intervals from the reservoir until total desorption of phenol. Adsorption-desorption cycles were performed many times using the same prepared adsorbent.

The desorption capacity of phenol was obtained at any cycle using the following equation:

$$q_e = \frac{(C_e)V}{m} \tag{2}$$

where V : volume of solution (mL); m : mass of adsorbent (g); C_e : equilibrium concentration of phenol in solution reservoir (mg/L).

3. Mathematical models

3.1. Isotherm models

Adsorption capacity of adsorbent is determined by using adsorption isotherm models. Freundlich and Langmuir are the most used to model adsorption processes in liquid phase. In 1918 Langmuir proposed a simple model of the adsorbent surface to derive an equation for an isotherm [44].

$$\frac{1}{q_e} = \frac{1}{q_0} + \frac{1}{bq_0} \frac{1}{C_e} \tag{3}$$

where q_e is the amount of adsorbate at equilibrium (mg/g), C_e is the concentration of the adsorbate at equilibrium (mg/L), and q_0 and b are the Langmuir constants. These constants can be determined, respectively, from the intercept and the slope of the linear plot of experimental data of $1/q_e$ vs. $1/C_e$.

Freundlich isotherm was introduced in 1926 [45]. The linear form of this model is given by the following relationship:

$$\ln q_e = \ln(k_F) + \frac{1}{n} \ln C_e \tag{4}$$

where k_F and n are Freundlich constants. The values of k_F and $1/n$ can be determined from the intercept and slope of the linear plot of experimental data of $\ln q_e$ vs. $\ln C_e$.

3.2. Kinetics of adsorption

Several kinetic adsorption models have been established to describe the adsorption kinetics. They include the second-order and pseudo-first-order models. In order to describe the kinetic process of adsorption of oxalic acid and malonic acid by charcoal. The first-order rate equation was presented by Lagergren in 1898 [46]. The general form of this model is expressed in:

$$\frac{dq_t}{dt} = k_1(q_e - q_t) \tag{5}$$

where q_t is the quantity adsorbed at any instant t , q_e is adsorbed amount of adsorbate at equilibrium (mg/g) and k_1 is the constant adsorption rate. Applying the boundary

conditions: $q_t = q_t$ at $t = t$ and $q_t = 0$ at $t = 0$ then integrating the equation, we obtain:

$$\ln(q_e - q_t) = \ln q_e - k_1 t \tag{6}$$

where k_1 and q_e can be obtained, respectively, from the slope and intercept between $\ln(q_e - q_t)$ as a function of time.

Kinetic process of divalent metal ions adsorption in peat surface was described by Ho et al. in 1995 [47]. The equation of second order speed can be written as follows:

$$\frac{dq_t}{dt} = k_2 [q_e - q_t]^2 \tag{7}$$

where k_2 is the constant adsorption rate, q_e is the amount adsorbed at equilibrium (mg/g), and q_t is the amount adsorbed at instant t (mg/g). Separating the variables and integrating the equation with the boundary conditions, $q_t = 0$ at $t = 0$ and $q_t = q_t$ at $t = t$, we obtain the following expression:

$$\frac{1}{q_e - q_t} = \frac{1}{q_e} + k_2 t \tag{8}$$

The rearrangement of the equation gives the equation in linear form:

$$\frac{t}{q_t} = \frac{1}{k_2} \frac{1}{q_e^2} + \frac{1}{q_e} t \tag{9}$$

Thus, by plotting the curve of t/q_t as a function of t , the values of k_2 , q_e can be determined.

For isothermal diffusion in a spherical adsorbent particle of radius, r , the sorption curve has been shown to follow the following equation:

$$\frac{q_t}{q_e} = 6 \sqrt{\frac{D_1 t}{r^2 \pi}} \tag{10}$$

where D is diffusivity of sorbate within the sorbent-pores (m^2/s), r is the radius of adsorbent particle, q_t is the amount of sorbate adsorbed from the sorbent surface at time t (mg/g of apatite) and q_e is the total amount of sorbate adsorbed on the sorbent surface (mg/g of adsorbent). Thus, by plotting the curve of q_t/q_e as a function of racine t , the values of D/r^2 can be determined [48].

4. Results and discussion

4.1. Characterization of the used adsorbent

Elemental analysis of the main constituent elements of HA and HA/SA is carried out using an ICP-AES

Table 1
Chemical composition of HA/SA and SA

Chemical elements (ppm)	Ca	P	Na	Cl
HA/SA	3,229.26	279.01	172.4	88.6
SA	2,571.44	6.92	97.93	44.3

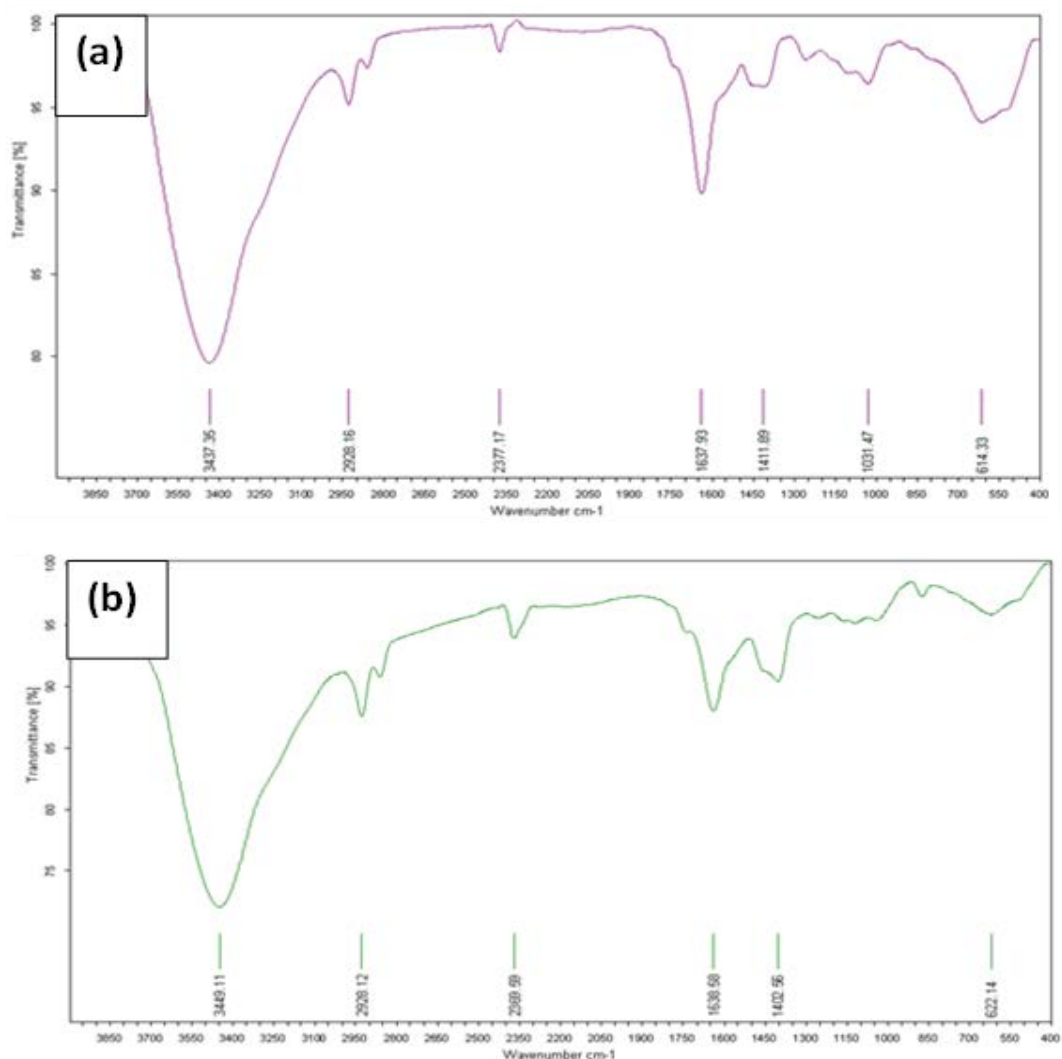


Fig. 2. Infrared spectrum of the adsorbent (HA/SA) (a) compared with SA (b).

diameter is of the order of a few micrometers. This deformation may be due to an entanglement of the macromolecular chains following the insertion of HA during the adsorbent preparation. Spectra of adsorbent show the presence of phosphate, which characterizes apatitic environments in addition to Ca and O, which are the major elements that constitute the structure of the polymer. The presence of Na⁺ and Cl⁻ is related to sodium alginate and calcium chloride used during the preparation of the adsorbent.

4.2. Effect of contact time

The results for the adsorption of phenol onto adsorbent as a function of time are shown in Fig. 4.

The adsorption equilibrium strongly depends on the initial concentration of phenol. Indeed, full 4 h are required to reach the equilibrium of adsorption reaction in the case of initial concentration of phenol equal to 100 mg/L, instead of only 30 min in the case of initial concentration of phenol equal to 60 mg/L.

4.3. Effect of adsorbent dose

We have varied adsorbent dose from 1.2 to 16 g/L. Fig. 5 shows the effect of adsorbent dosage on adsorption capacity of phenol. Results obtained show that the phenol removal increases as the adsorbent dose increases and reaches a maximum value at 12 g/L of adsorbent. Hence, optimum adsorbent dose is considered as 12 g/L of adsorbent. This result may be due to the increase of the adsorbent surface area. However any increase in adsorbent dose more than the optimum value does not have significantly improved the adsorption capacity because the equilibrium between phenol ions and the adsorbent surface was reached.

4.4. Effect of temperature

Fig. 6 shows that increasing the temperature between 20°C and 60°C, slightly decreases the adsorption capacity of the phenol, which means the adsorption reaction could be

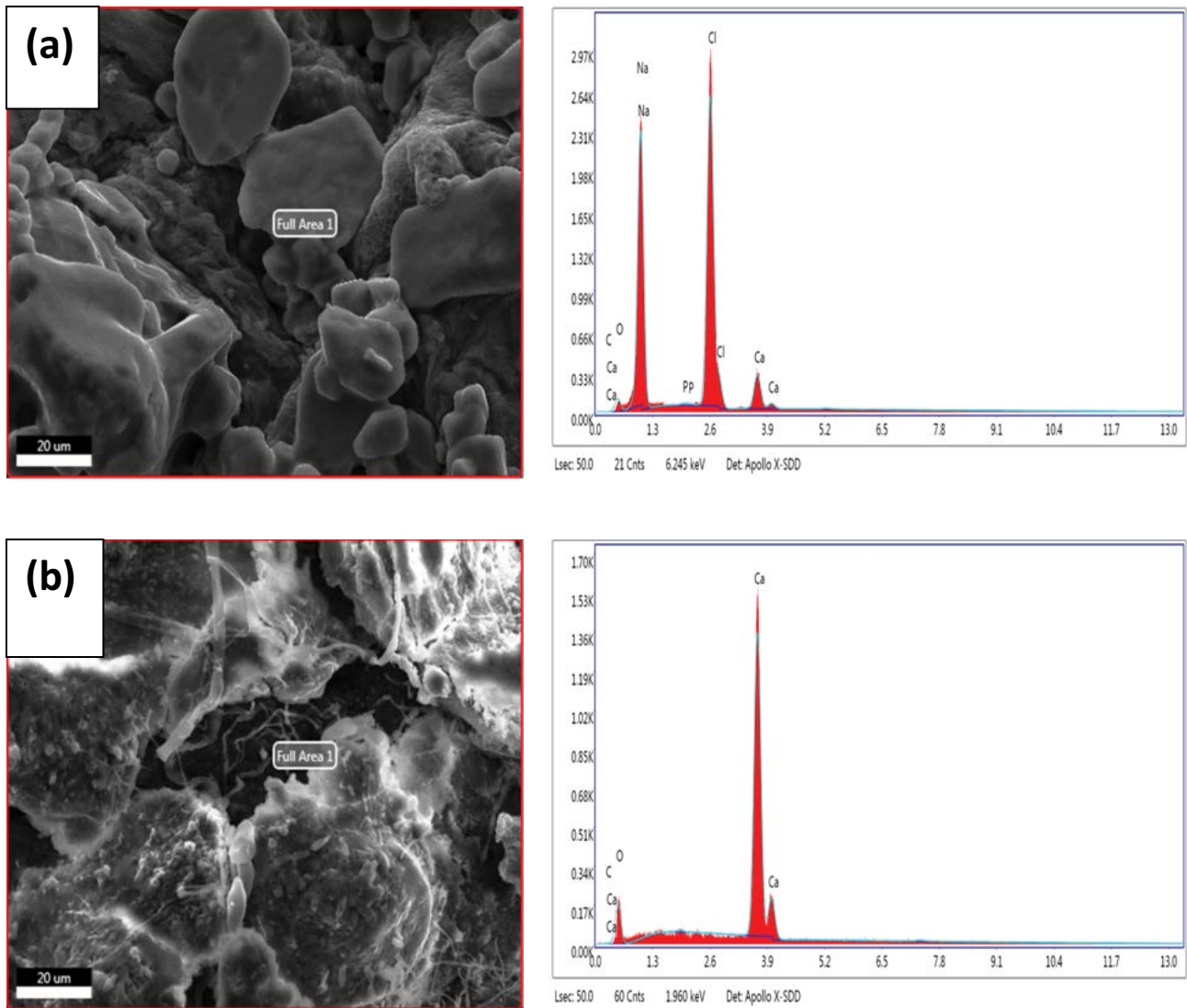


Fig. 3. SEM images coupled energy-dispersive X-ray analysis of HA/SA (a) compared with SA (b).

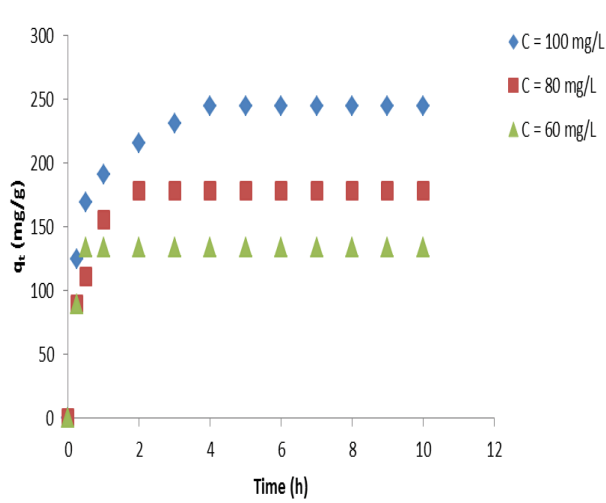


Fig. 4. Kinetic study of adsorption of phenol onto HA/SA at different initial concentration of phenol.

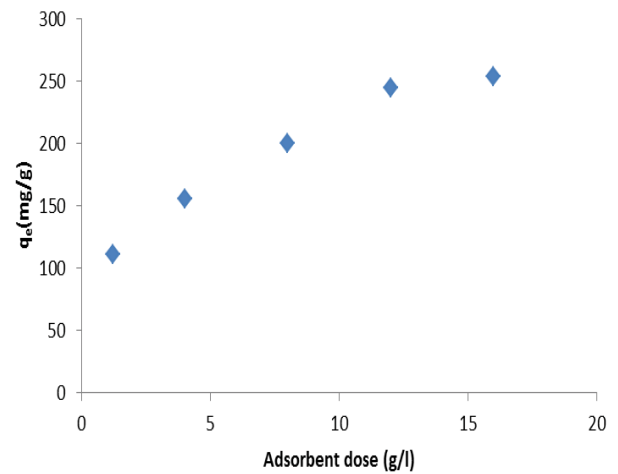


Fig. 5. Effect of the adsorbent dose on adsorption capacity of phenol (phenol initial concentration = 100 mg/L, pH = 6.20 at room temperature).

exothermic [38]. This behavior could be explained by the vibrational energies of the adsorbed phenol molecules at high temperature; these molecules are more likely to desorb from adsorbent surface, which leads to a decrease in the adsorption capacity [47].

4.5. Effect of pH

The effect of pH on capacity adsorption of phenol on HA/SA is a very important parameter. The results displayed in Fig. 7 show a low adsorption value at pH = 3 and the adsorption capacity increases as the pH increases to the value of pH = 6.2, above this value, the adsorption capacity decreases progressively with increasing pH value. This can be related to the phenol ionization, in acid state, positive charge is dominant on adsorbent surface (pH

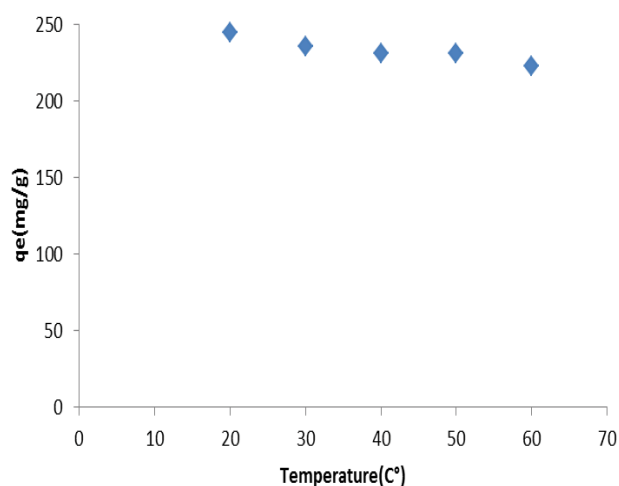


Fig. 6. Effect of temperature on the capacity adsorption of phenol onto HA/SA (phenol initial concentration = 100 mg/L at pH = 6.20).

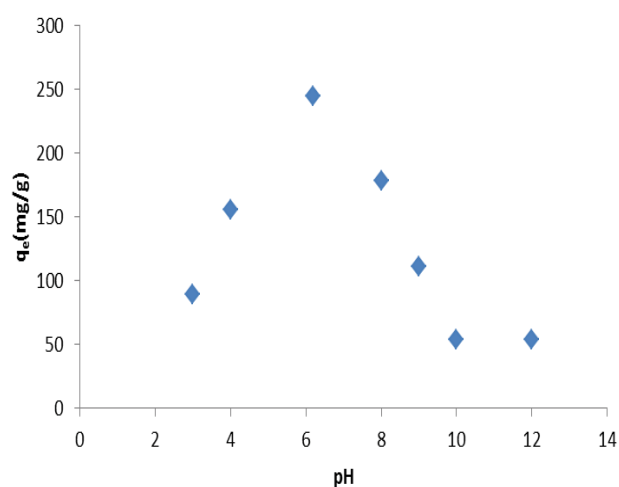


Fig. 7. Effect of pH of solution on the adsorption capacity of phenol on HA/SA (phenol initial concentration = 100 mg/L at room temperature).

of zero charge of adsorbent equal to 6) and thus a high electrostatic attraction exists between positive charges of adsorbent surface and negative charges of phenolates formed, which promotes the adsorption phenomenon. In the alkaline state, dominant charge of adsorbent surface is negative and phenol as a weak acid with $pK_a = 9.89$ is dissociated at value of $pH > pK_a$. Therefore, the adsorption decreases at high pH values related to the electrostatic repulsions existing between the negative surface charge and the phenolate anions carrying the same charge as the adsorbent surface. It could be also due to the electrostatic repulsion between phenolate ions themselves, similar behavior has been reported by other authors [47].

4.6. Adsorption isotherms

Adsorption isotherms are important to describe the interaction between phenol ions and adsorbent surface and also for optimization of the use of these materials as adsorbents. Fig. 8 gives the evolution of the amount of adsorbed phenol as a function of phenol concentration at equilibrium. The obtained isotherm is of type C according to the classification of Giles et al. [50], the linearity of the curve shows that the number of sites during adsorption reaction remains constant. That means as more phenol ions are adsorbed more sites in adsorbent surface must be created. Results show also that the adsorption capacity increases progressively with initial concentration of phenol, which is related to the increase in the collision between phenol ions and adsorbent surface. The same result was found by Oumani et al. [51] in a study of removal of Cr^{3+} from tanning effluent by adsorption onto phosphate mine waste. Linear representations of experimental values of adsorption capacity of phenol ions on the adsorbent according to Langmuir and Freundlich models give straight lines (Figs. 9 and 10) whose constants are grouped in Table 2. According to the correlation coefficient (R^2) of the lines obtained by these models, we conclude that Freundlich model is the most likely to characterize this

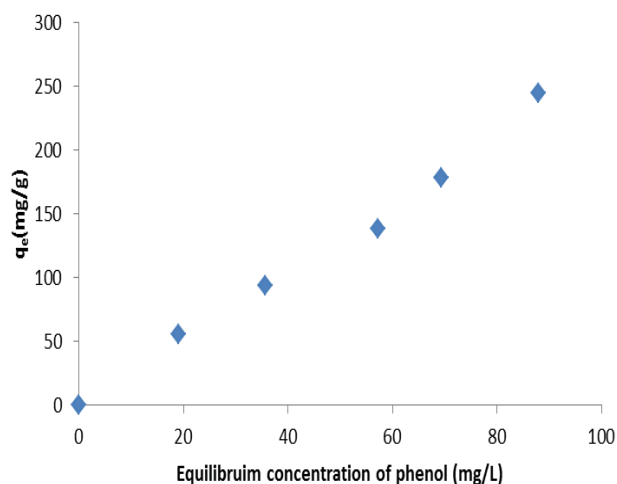


Fig. 8. Influence of equilibrium concentration of phenol on the adsorption capacity of phenol on HA/SA (pH = 6.20 at room temperature).

adsorption mechanism. The maximum experimental adsorption capacity value determined for phenol onto HA/SA is higher than those reported for other adsorbents (Table 3).

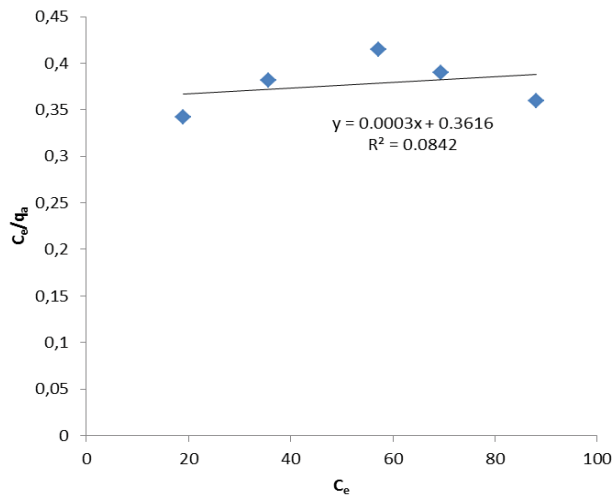


Fig. 9. Langmuir plot for phenol adsorption onto HA/SA.

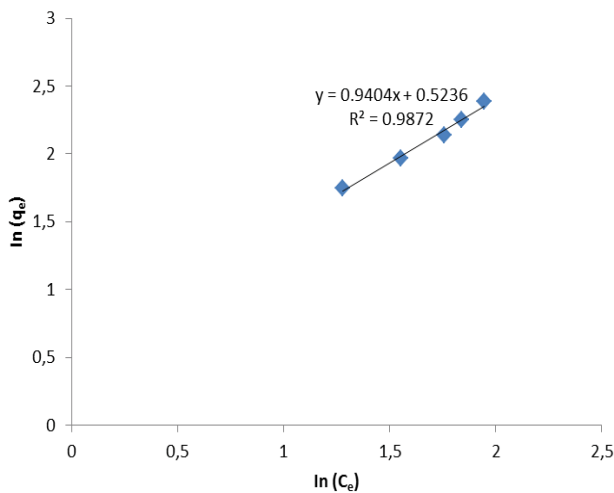


Fig. 10. Freundlich plot for phenol adsorption onto HA/SA.

Table 3
Comparison of the HA/SA adsorption capacity with other adsorbents

Adsorbent	Phenol initial concentration (mg/L)	Adsorption capacity (mg/g)	Reference
Natural phosphate (NP)	40	23	[38]
Hydroxyapatite (Hap)	100	8	[39]
Sedimentary phosphate (SP)	100	40	[40]
Pecan shells AC	35	18	[52]
Coffee residue AC	170	84.02	[53]
Black stone cherries AC	500	133.33	[54]
Natural phosphate (NP)	100	12	[55]
Hydroxyapatite-calcium alginate composite (HA/SA)	100	244	

4.7. Adsorption kinetics studies

The variation of adsorption capacity of phenol onto HA/SA as a function of time is shown in Fig. 11. The examination of the curve obtained shows that the kinetics of phenol adsorption is very slow compared with adsorption of phenol from aqueous solutions by other adsorbents reported in the literature [39]. Indeed, the adsorption reaction appears to be a two-step process. In the first hour, the adsorption capacity increased rapidly (78%), After this initial fast adsorption period, the adsorption of phenol reaches the adsorption equilibrium in about 4 h. This slow kinetic can be related to the structure of the adsorbent, which constitutes of many pore and deformation due to entanglement of the macromolecular chains following the insertion of apatite during preparation step of the adsorbent. Kinetic models of pseudo-first-order, second order and pore diffusion have been investigated.

The analyses of the obtained curves (Figs. 12–14) show that the adsorption reaction of phenol ions on the adsorbent can be described by the pseudo-second-order model. Adsorption kinetic parameters are calculated and are summarized in Table 4. The correlation coefficient value (R^2) for the pseudo-second-order model is higher than those for the first order kinetic and pore diffusion. The theoretical values of adsorbed phenol amount at equilibrium ($q_{e,cal}$) are close to the experimental values ($q_{e,exp}$) (Table 4).

4.8. Adsorption–regeneration

Results for phenol desorption from the tested adsorbent as a function of time are shown in Fig. 15. Analysis of the curve shows that the desorption reaction of phenol ions is a two-step reaction like adsorption process. In the first hour, the desorption capacity increased rapidly (64%), after this

Table 2
Characteristic parameters of phenol adsorption according to Langmuir and Freundlich models

Langmuir isotherm			Freundlich isotherm		
q_0 (mg/g)	b	R^2	n	k_F	R^2
3,334	0.0008	0.08	1.06	1.68	0.99

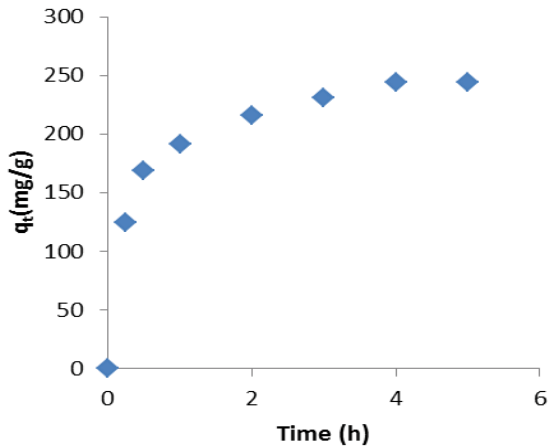


Fig. 11. Effect of contact time on adsorption capacity of phenol on HA/SA (phenol initial concentration = 100 mg/L and stirring time = 24 h at pH = 6.20 and room temperature).

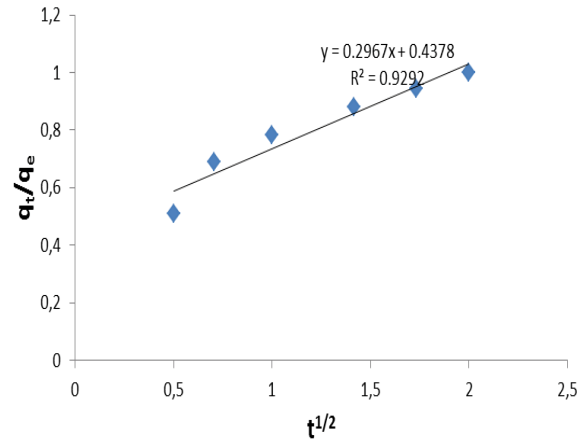


Fig. 14. Pore diffusion model plot for phenol adsorption onto HA/SA.

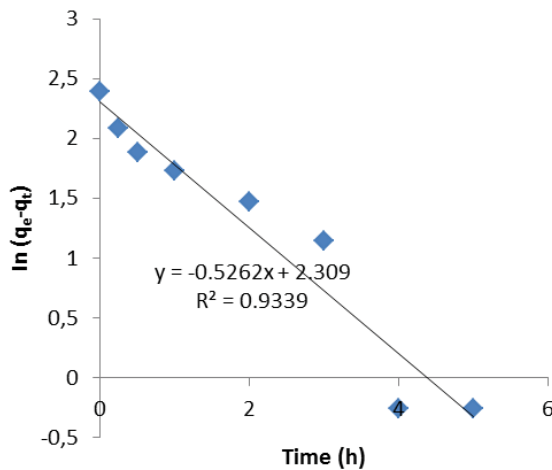


Fig. 12. Pseudo-first-order kinetic plots for phenol adsorption onto HA/SA.

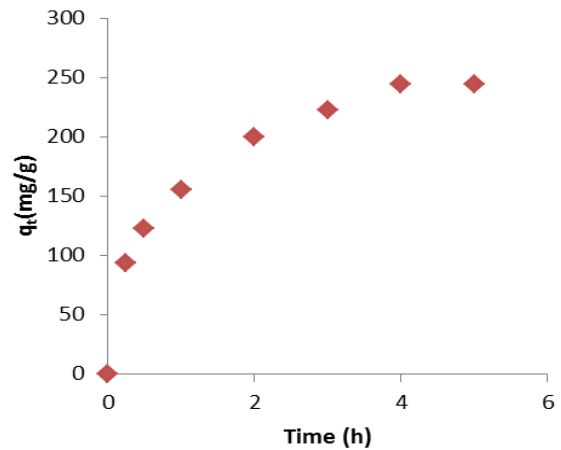


Fig. 15. Effect of contact time on desorption of phenol by HA/SA (phenol initial concentration = 100 mg/L, pH = 6.20 at room temperature).

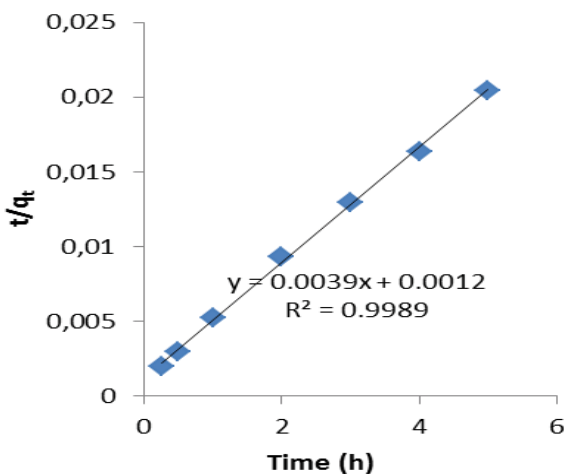


Fig. 13. Pseudo-second-order plots for phenol adsorption onto HA/SA.

initial fast desorption period, the regeneration of phenol reaches the desorption equilibrium in about 4 h. In order to better describe the mechanism of reaction desorption, it was necessary to propose a suitable model for desorption of phenol. For this purpose, pore diffusion, pseudo-first-order and pseudo-second-order kinetics were applied (Figs. 16–18), desorption reaction of phenol ions from the adsorbents can be described by an equation corresponding to the pseudo-second-order model and pore diffusion. The desorption kinetic parameters were calculated and are summarized in Table 5. The theoretical values of amount of adsorbed phenol at equilibrium ($q_{e,cal}$) are close to the experimental values ($q_{e,cal}$) (Table 5).

4.9. Reusability of adsorbent

In order to understand the reusability of the used adsorbent, we have carried out many cycles of adsorption-desorption. Results are shown in Fig. 19. For six cycles of

Table 4
Characteristic parameters of the phenol adsorption according to the pseudo-second-order

Pseudo-first-order model				Pseudo-second-order model			Pore diffusion model	
$q_{e,cal}$ (mg/g)	k_1 (1/h)	$q_{e,cal}$ (mg/g)	R^2	k_2 (g/mg h)	$q_{e,cal}$ (mg/g)	R^2	D	R^2
244	0.52	10	0.92	0.012	256	0.99	67.7	0.92

Table 5
Characteristic parameters of the phenol desorption according to the pseudo-second-order model, the pseudo-first-order model and pore diffusion model

Pseudo-first-order model			Pseudo-second-order model			Pore diffusion model	
k_1 (h)	$q_{e,cal}$ (mg/g)	R^2	k_2 (g/mg h)	$q_{e,cal}$ (mg/g)	R^2	D	R^2
0.52	11	0.91	0.0054	277	0.99	60.96	0.99

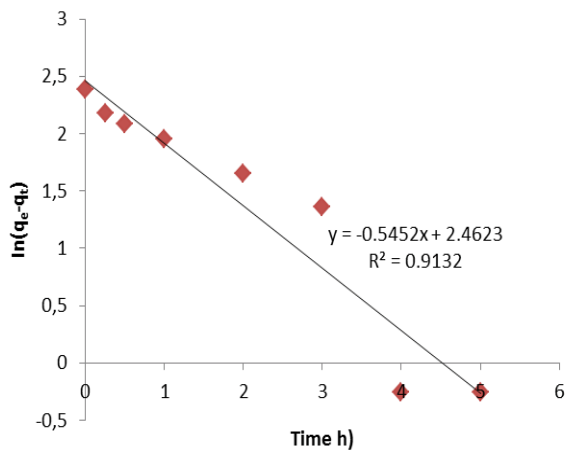


Fig. 16. First-order kinetic plots for phenol desorption onto HA/SA.

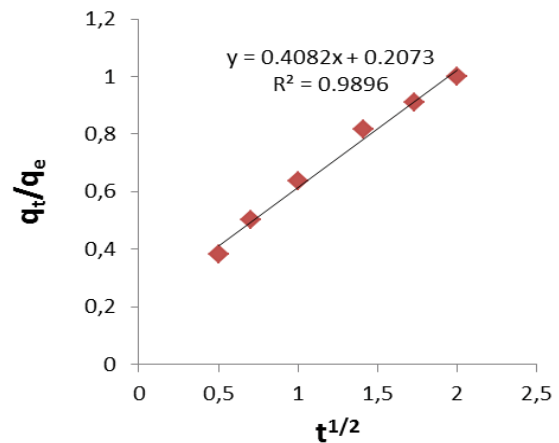


Fig. 18. Pore diffusion model plots for phenol desorption onto HA/SA.

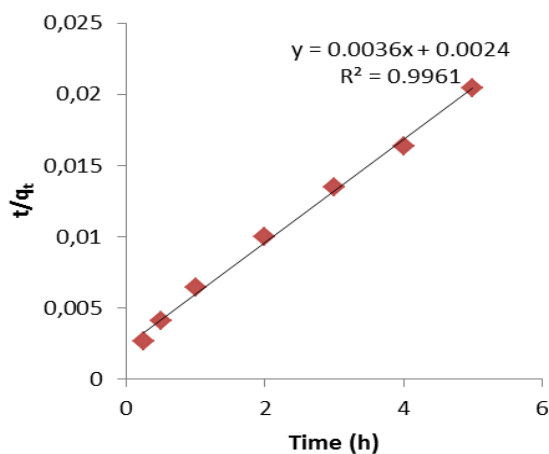


Fig. 17. Pseudo-second-order plots for phenol desorption onto HA/SA.

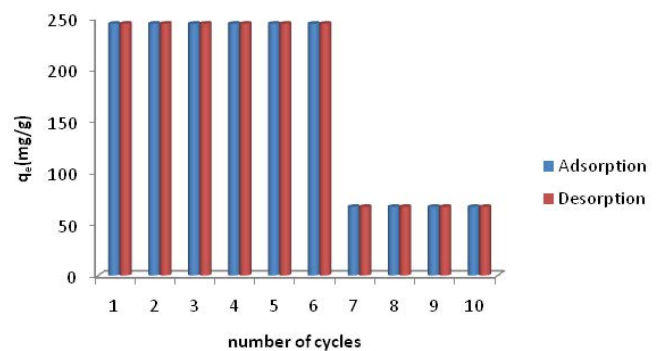


Fig. 19. Cycle number effect of adsorption/desorption on adsorption capacity of phenol.

adsorption–desorption, the adsorbent kept its high adsorption capacity, from the seventh cycle, the adsorption capacity decreases from 244 to 60 mg/g, which is related to saturation of adsorption sites.

5. Conclusion

In conclusion, we herein reported the successful synthesis of a green and efficient adsorbent (HA/SA) through a cross-linking process. The resulting adsorbent was characterized by SEM and FTIR showing its interesting properties. In addition, adsorption experiments confirmed

that the adsorption reaction of phenol ions onto the synthesised adsorbent was highly dependent on pH, adsorbent dosage, initial phenol concentration, with a maximum adsorption capacity of 244 mg/g at 25°C and pH equal 6.2. The exploitation of the adsorption isotherm indicates a best fit with the Freundlich model and kinetic investigations demonstrated that the adsorption data are more correlated with a pseudo-second-order model. Finally, results of phenol regeneration shows that adsorbed phenol remains almost unstable and can be desorbed from HA/SA using only distilled water. After six cycles of adsorption-desorption processes, the adsorbent kept its high adsorption capacity that decreases at the seventh cycle, to 60 mg/g, due to non-reversible saturation of adsorption sites.

References

- [1] S. Rengaraj, S.H. Moon, R. Sivabalan, B. Arabindoo, V. Murugesan, Removal of phenol from aqueous solution and resin manufacturing industry wastewater using an agricultural waste: rubber seed coat, *J. Hazard. Mater.*, 89 (2002) 185–196.
- [2] L. Jakobek, Interactions of polyphenols with carbohydrates, lipids and proteins, *Food Chem.*, 175 (2015) 556–567.
- [3] M. Samimi, M. Shahriari Moghadam, Phenol biodegradation by bacterial strain O-CH1 isolated from seashore, *Global J. Environ. Sci. Manage.*, 6 (2020) 109–118.
- [4] M. Shahriari Moghadam, N. Safaei, G.H.E. brahimipour, Optimization of phenol biodegradation by efficient bacteria isolated from petrochemical effluents, *Global J. Environ. Sci. Manage.*, 2 (2016) 249–256.
- [5] L. Zhou, J. Hu, H. Zhong, X. Li, Study of phenol removal using fluidized-bed Fenton process, *Chem. Eng. Res. Des.*, 90 (2012) 377–382.
- [6] O. Sacco, V. Vaiano, Ch. Daniel, W. Navarra, V. Venditto, Removal of phenol in aqueous media by N-doped TiO₂ based photocatalytic aerogels, *Mater. Sci. Semicond. Process.*, 80 (2018) 104–110.
- [7] M.F. Abid, O.N. Abdulla, A.F. Kadhim, Study on removal of phenol from synthetic wastewater using solar photo catalytic reactor, *J. King Saud Univ. Eng. Sci.*, 31 (2019) 131–139.
- [8] B. Chokri, Kh. Moncef, M. Salma, K. Monem, E. Boubaker, F. Jean Francois, Electrochemical treatment of olive mill wastewater: treatment extent and effluent phenolic compounds monitoring using some uncommon analytical tools, *J. Environ. Sci.*, 25 (2013) 220–230.
- [9] E. Ouabou, A. Anouar, S. Hilali, Traitement de la margine brute d'huile d'olive par distillation suivi de neutralisation par chaux, *J. Appl. Biosci.*, 79 (2014) 6867–6872.
- [10] G. Sbai, M. Loukili, Traitement des margines par un procédé-couplant la coagulation floculation et la voie électrochimique, *Eur. Sci. J.*, 11 (2015) 1857–7881.
- [11] O. Chedeville, M. Debacq, C. Porte, Removal of phenolic compounds present in olive mill wastewaters by ozonation, *Desalination*, 24 (2009) 865–869.
- [12] M. Achak, N. Ouazzani, L. Mandi, Treatment of modern olive mill effluent by infiltration-percolation on a sand filter, *Rev. Des Sci. De L'Eau*, 22 (2009) 421–433.
- [13] W. Raza, J. Lee, N. Raza, Y. Luo, K.-H. Kim, J. Yang, Removal of phenolic compounds from industrial waste water based on membrane-based technologies, *J. Ind. Eng. Chem.*, 71 (2019) 1–18.
- [14] M.D. Víctor-Ortega, J.M. Ochando-Pulido, A. Martínez-Ferez, Phenols removal from industrial effluents through novel polymeric resins: kinetics and equilibrium studies, *Sep. Purif. Technol.*, 160 (2016) 136–144.
- [15] C. Datta, A. Dutta, D. Dutta, S. Chaudhuri, Adsorption of polyphenols from ginger rhizomes on an anion exchange resin Amberlite IR-400-Study on effect of pH and temperature, *Procedia Food Sci.*, 1 (2011) 893–899.
- [16] Ö. Aktaş, F. Çeçen, Adsorption, desorption and bioregeneration in the treatment of 2-chlorophenol with activated carbon, *J. Hazard. Mater.*, 141(2007) 769–777.
- [17] S.J. Kulkarni, R.W. Tapre, S.V. Patil, M.B. Sawarkar, Adsorption of phenol from wastewater in fluidized bed using coconut shell activated carbon, *Procedia Eng.*, 51 (2013) 300–307.
- [18] M.A. Dabhade, M.B. Saidutta, D.V.R. Murthy, Adsorption of phenol on granular activated carbon from nutrient medium: equilibrium and kinetic study, *Int. J. Environ. Res.*, 3 (2009) 557–568.
- [19] N.T. Abdel-Ghani, G.A. El-Chaghaby, F.S. Helal, Preparation, characterization and phenol adsorption capacity of activated carbons from African beech wood sawdust, *Global J. Environ. Sci. Manage.*, 2 (2016) 209–222.
- [20] S. Zeboudj, M. Loucif Seiad, A. Namane, D. Hank, A. Hellal, Elimination du phenol: couplage de l'adsorption sur charbon actif et la biodegradation par *Pseudomonas aeruginosa*, *Rev. Microbiol. Ind. San et Environn.*, 8 (2014) 1–15.
- [21] B. Ozkaya, Adsorption and desorption of phenol on activated carbon and comparison of isotherm models, *J. Hazard. Mater.*, 129 (2006) 158–163.
- [22] F. Belaib, A.H. Meniai, M.B. Lehocine, Elimination of phenol by adsorption onto mineral/polyaniline composite solid support, *Procedia Eng.*, 18 (2012) 1254–1260.
- [23] A. El Gaidoumi, A.Ch. benabdallah, A. lahrichi, A. kherbeche, Adsorption of phenol in aqueous medium by a raw and treated Moroccan pyrophyllite, *J. Mater. Environ. Sci.*, 6 (2015) 2247–2259.
- [24] C.R. Girish, V. Ramachandra Murty, Adsorption of phenol from wastewater using locally available adsorbents, *J. Environ. Res. Develop.*, 6 (2012) 763–772.
- [25] M. Achak, A. Hafidi, N. Ouazzani, S. Sayadi, L. Mandi, Low cost biosorbent “banana peel” for the removal of phenolic compounds from olive mill wastewater: kinetic and equilibrium studies, *J. Hazard. Mater.*, 166 (2009) 117–125.
- [26] S. Elabbas, L. Mandi, F. Berrekhis, M.N. Pons, J.P. Leclerc, N. Ouazzani, Removal of Cr(III) from chrome tanning waste water by adsorption using two natural carbonaceous materials: eggshell and powdered marble, *J. Environ. Manage.*, 166 (2016) 589–595.
- [27] B.M. Villar da Gama, G. Elisandra do Nascimento, D.C. Silva Sales, J.M. Rodríguez-Díaz, C.M. Bezerra De Menezes Barbosa, M.M. Menezes Bezerra Duarte, Mono and binary component adsorption of phenol and cadmium using adsorbent derived from peanut shells, *J. Cleaner Prod.*, 201 (2018) 219–228.
- [28] L. Sellaoui, M. Kehili, E.C. Lima, P.S. Thue, A. Bonilla-Petriciolet, A. Ben Lamine, G.L. Dotto, A. Erto, Adsorption of phenol on microwave-assisted activated carbons: modelling and interpretation, *J. Mol. Liq.*, 274 (2019) 309–314.
- [29] I. Ali, M. Asim, T.A. Khan, Low cost adsorbents for the removal of organic pollutants from wastewater, *J. Environ. Manage.*, 113 (2012) 170–183.
- [30] V.K. Gupta, I. Ali, Chapter 2 – Water Treatment for Inorganic Pollutants by Adsorption Technology, In: *Environmental Water, Advances in Treatment, Remediation and Recycling*, Elsevier, 2013, pp. 29–91.
- [31] S. De Gisi, G. Lofrano, M. Grassi, M. Notarnicola, Characteristics and adsorption capacities of low-cost sorbents for wastewater treatment: a review, *SM&T*, 9 (2016) 10–40.
- [32] M. Moradi, M. Heydari, M. Darvish motevalli, K. Karimyan, V.K. Gupta, Y. Vasseghian, H. Sharafi, Kinetic and modeling data on phenol removal by Iron-modified Scoria Powder (FSP) from aqueous solutions, *Data Brief*, 20 (2018) 957–968.
- [33] H. Bensalah, M.F. Bekheet, S.A. Younssi, M. Ouammou, A. Gurlo, Hydrothermal synthesis of nanocrystalline hydroxyapatite from phosphogypsum waste, *J. Environ. Chem. Eng.*, 6 (2018) 1347–1352.
- [34] S. Saoiabi, A. Gouza, H. Bouyarmane, A. Laghzizil, A. Saoiabi, Organophosphate-modified hydroxyapatites for Zn(II) and Pb(II) adsorption in relation of their structure and surface properties, *J. Environ. Chem. Eng.*, 4 (2016) 428–433.

- [35] H. Bachoua, H. Nasri, M. Debbabi, B. Badraoui, Using tunisian phosphate rock and her converted hydroxyapatite for lead removal from aqueous solution, *Int. J. Eng. Res. Appl.*, 4 (2014) 171–178.
- [36] H. Bouyarmane, S. Saoiabi, A. Laghzizil, A. Saoiabi, A. Rami, M. El Karbane, Natural phosphate and its derivative porous apatite adsorbents: kinetic process and impact of the surface properties, *Desal. Water Treat.*, 5 (2013) 7265–7269.
- [37] A. Bahdod, S. El Asri, A. Saoiabi, T. Coradin, A. Laghzizil, Adsorption of phenol from an aqueous solution by selected apatite adsorbents: kinetic process and impact of the surface properties, *Water Res.*, 43 (2009) 313–318.
- [38] A.S. Alzaydien, W. Manasreh, Equilibrium, kinetic and thermodynamic studies on the adsorption of phenol onto activated phosphate rock, *Int. J. Phys. Sci.*, 4 (2009) 172–181.
- [39] H. Bouyarmane, S. El Asri, A. Rami, C. Roux, M.A. Mahly, A. Saoiabi, T. Coradin, A. Laghzizil, Pyridine and phenol removal using natural and synthetic apatite as low cost sorbents: influence of porosity and surface interactions, *J. Hazard. Mater.*, 181 (2010) 736–741.
- [40] H. Yaacoubi, Z. Songlin, M. Mouflih, M. Gourai, S. Sebti, Adsorption isotherm, kinetic and mechanism studies of 2-nitrophenol on sedimentary phosphate, *Mediterr. J. Chem.*, 4 (2015) 289–296.
- [41] W. Tanthapanichakoon, P. Ariyadejwanich, P. Japthong, K. Nakagawa, S.R. Mukai, H. Tamon, Adsorption–desorption characteristics of phenol and reactive dyes from aqueous solution on mesoporous activated carbon prepared from waste tires, *Water Res.*, 39 (2005) 1347–1353.
- [42] S. El Asri, A. Laghzizil, A. Saoiabi, A. Alaoui, K. El Abassi, R. M'hamdi, A novel process for the fabrication of nanoporous apatites from Moroccan phosphate rock, *Colloids Surf. A*, 350 (2009) 73–78.
- [43] F. Aziz, M. El Achaby, A. Lissaneddine, Kh. Aziz, N. Ouazzani, R. Mamouni, L. Mandi, Composites with alginate beads: a novel design of nano-adsorbents impregnation for large-scale continuous flow wastewater treatment pilots, *Saudi J. Biol. Sci.*, 27 (2020) 2499–2508.
- [44] I. Langmuir, J. Amer, The adsorption of gases on planes of glass mica and platinum, *J. Am. Chem. Soc.*, 40 (1918) 1361–1403.
- [45] H. Freundlich, *Colloid and capillary chemistry*, *J. Chem. Educ.*, 3 (1926) 1454.
- [46] H. Qiu, L. Lv, B.-c. Pan, Q.-J. Zhang, W.-M. Zhang, Q.-x. Zhang, review in adsorption kinetic models, *J. Zhejiang Univ. Sci. A*, 10 (2009) 716–724.
- [47] M. Loredo-Cancino, E. Soto-Regalado, R.B. García-Reyes, F. de j. Cerino-Córdova, M.T. Garza-González, M. M. Alcalá-Rodríguez, N.E. Dávila-Guzmán, Adsorption and desorption of phenol onto barley husk-activated carbon in an airlift reactor, *Desal. Water Treat.*, 1 (2014) 1–16.
- [48] D.M. Ruthven, *Principles of Adsorption and Adsorption Processes*, Wiley and Sons, New York, 1984.
- [49] G.C. Fontes, V.M.A. Calado, A.M. Rossi, M.H.M. da Rocha-Leão, Characterization of antibiotic-loaded alginate-Osa starch microbeads produced by ionotropic pregelation, *J. Biomed. Biotechnol.*, (2013) 1–11 (Special Issue).
- [50] C.H. Giles, T.H. MacEwan, S.N. Nakhwa, D. Smith, A system of classification of solution adsorption isotherms, and its use in diagnosis of adsorption mechanisms and in measurement of specific surface areas of solids, *J. Chem. Soc.*, 786 (1960) 3973–3993.
- [51] A. Oumani, L. Mandi, F. Berrekhis, N. Ouazzani, Removal of Cr³⁺ from tanning effluents by adsorption onto phosphate mine waste: key parameters and mechanisms, *J. Hazard. Mater.*, 378 (2019) 120718.
- [52] R.A. Shawabkeh, E.S.M. Abu-Nameh, Absorption of phenol and methylene blue by activated carbon from pecan shells, *Colloid J.*, 69 (2007) 355–359.
- [53] L. Khenniche, F. Benissad-Aissani, Adsorptive removal of phenol by coffee residue activated carbon and commercial activated carbon: equilibrium, kinetics, and thermodynamics, *J. Chem. Eng. Data*, 55 (2010) 4677–4686.
- [54] J.M.R. Rodriguez Arana, R.R. Mazzoco, Adsorption studies of methylene blue and phenol onto black stone cherries prepared by chemical activation, *J. Hazard. Mater.*, 180 (2010) 656–661.
- [55] R. Benaddi, Kh. El harfi, F. Aziz, F. Berrekhis, N. Ouazzani, Removal of phenolic compounds from synthetic solution and oil mill waste water by adsorption onto nanoparticles synthesized from phosphate rock, *J. Surface Sci. Technol.*, 36 (2020) 39–51.